Supporting Informaiton

Rucci et al. 10.1073/pnas.0914865107

SI Materials and Methods

Immunophenotypic Analysis. Immunophenotypic analysis of T and B cell populations was performed using the following anti-mouse antibodies: APC-conjugated anti-CD4, biotin-conjugated anti-CD8, biotin-conjugated anti-CD4, PerCP-conjugated anti-CD4, FITC-conjugated anti-CD3, biotin-conjugated anti-B220, biotin-conjugated anti-CD11b, biotin-conjugated anti-Gr1, FITC-conjugated anti-CD44, PE-conjugated anti-CD25, PE-conjugated anti-CD62L, FITC- and APC-conjugated anti-B220, FITC-conjugated anti-CD43, and PerCp- and APC-conjugated anti-IgM (all from BD Biosciences); PE-conjugated anti-CD8, Alexa700-conjugated anti-B220, Pacific Blue-conjugated anti-IgD, PE-conjugated anti-AA4.1, PE-Cy7-conjugated anti-CD23, PE-Cy5-conjugated anti-IgM, APC-conjugated anti-GL7, and the APC anti-mouse Foxp3 staining set (all from eBioscience); and APC-conjugated-anti-CD24 (clone M1/69) and FITC-conjugated anti-IgG1 (Biolegend). Samples stained with biotin-conjugated antibodies underwent an additional incubation with PerCp-conjugated streptavidin (BD Pharmingen). $B220^+$ B cell subpopulations in the spleen were defined as follows:

Transitional (Tr1-Tr2) B cells: $AA4.1^+$ $B220^+$ IgM^{hi} $CD21^{lo}$
Follicular B cells: $AA4.1^-$ $B220^+$ $CD21^{int}$ IgD^+ $CD23^+$
Marginal zone B cells: $AA4.1^-$ $B220^+$ $CD21^{hi}$ $CD23^-$ IgM^{hi}
IgG1-producing cells: $B220^{hi}$ $^+$ $icIgG1^+$.

Histopathology. Histopathology of the thymus was performed on five 4- to 6-week-old mice, whereas search for lymphoid infiltrates in the liver and the gut was performed on five 8-week-old mice. Four-micrometer-thick sections from formalin-fixed, paraffin-embedded tissues were taken on a microtome and subjected to routine hematoxylin/eosin staining. For immunohistochemistry, sections were dewaxed and rehydratated through serial passages in xylene and alcohol and endogenous peroxidase activity was blocked with 0.3% H_2O_2 in methanol. Epitope retrieval was achieved by microwave treatment in PBS buffer containing 1.0 mM EDTA buffer, pH 8.0. Sections were then washed and incubated for 20 min in 5% normal human serum before incubation for 2 h with the primary antibody (rat polyclonal anti-mouse CD3, DAKO Cytomation), followed by 30 min incubation in buffer containing the appropriate secondary antibody (biotinylated rabbit anti-rat, 1:100, Vector). Immunolabeling was then revealed by incubation with streptavidin–horseradish peroxidase (HRP) and diaminobenzidine (DAB) (DAKO Cytomation) and slides were counterstained with hematoxylin. Images were acquired with an Olympus DP70 digital camera mounted on an Olympus Bx60 microscope, using $Cell^F$ imaging software (Soft Imaging System).

Analysis of T and B Cell Repertoire. For analysis of T cell repertoire, cDNA was prepared by reverse transcriptase using RNA from thymocytes and from T cell-enriched splenocytes, positively selected using anti-CD90 mAb-coated magnetic beads (Miltenyi Biotec). Immunoscope analysis of TCR Vβ repertoire was performed as described (1). Briefly, 2 ng of cDNA was amplified with each of the 24 TCRVβ family member-specific primers together with a TCRCβ primer. Amplification was performed for 40 cycles at 60 °C of annealing temperature and 1 min 30 sec of extension, using TaqGold (Applied Biosystems). Each PCR product (5 μL) was then subjected to four runoff reactions using a nested fluorescent primer specific for the TCRCβ segment. Runoff conditions were as follows: 2 min at 94 °C, 2 min at 60 °C, and 20 min at 72 °C.

For the analysis of B cell repertoire, cDNA was prepared from B cell-enriched splenocytes, obtained following negative selection using anti-CD90-coated magnetic beads (Miltenyi Biotec). The following primers were used to amplify the CDR3 region of Ig heavy chains:

Forward primers:

MIGHV1: 5′-TCCAGCACAGCCTACATGCAGCTC-3′
MIGHV2: 5′-CAGGTGCAGCTGAAGGAGTCAGG-3′
MIGHV3: 5′-AGGTGCAGCTTCAGGAGTCAGG-3′
MIGHV5: 5′-CAGCTGGTGGAGTCTGGGGGA-3′
MIGHV6: 5′-AAGTGAAGCTTGAGGAGTCTGG-3′
MIGHV7: 5′-AGGTGAAGCTGGTGGAGTCTGG-3′.

Reverse primer:

MIGH J_H: 5′-CTTACCTGAGGAGACGGTGA-3′.

Amplification reactions were performed using 2 ng of cDNA in 50 μL of reaction containing 1 unit/μL of Taq DNA polymerase modified for hot-start PCR, 200 μM dNTPs, 1 μM of each primer, and 1.5 mM $MgCl_2$ in 10× amplification buffer (Applied Biosystems). After initial incubation for 10 min at 95 °C, the amplification was carried out for 40 cycles as follows: 30 sec at 94 °C, 30 sec at 60 °C, and 1 min 30 sec at 72 °C, followed by a final step of 10 min at 72 °C. Each PCR product was subjected to 4 runoff cycles primed with the same reverse primer used for the PCR and labeled with 6-carboxyfluorescein (0.2 μM) in the presence of 1 unit/μL of Taq DNA polymerase modified for hot-start PCR, 200 μM dNTPs, and 1.5 mM $MgCl_2$ in 10× amplification buffer. Runoff cycles were as follow: 2 min at 94 °C, 2 min at 60 °C, and 20 min at 72 °C. PCR products were then processed on an ABI3130 genetic analyzer. Spectratype data were analyzed using GeneMapper v3.7 software.

Analysis of Cytokine Production. Splenic T cells were cultured in vitro for 72 h with anti-CD3 plus anti-CD28 mAb as detailed above. At the end of the culture, the supernatants were collected and analyzed using Multiplex Bead Immunoassays for cytokines of interest (IL-2, IL-4, IL-5, IL-6, IL-10, IL-13, IL-17, IFN-γ, and TNF-α), following the manufacturer's instructions (Invitrogen) and using a Luminex IS 100 instrument. Data were analyzed using the Luminex 100 Integrated System 2.3 software and were reported as median fluorescent intensity.

Measurement of Specific Antibodies. Low- and high-affinity anti-TNP IgG antibody titers were measured by ELISA 7 days after secondary immunization with TNP-KLH, by using plates that had been precoated with TNP(11)-BSA and with TNP(2)-BSA, respectively. Anti-single-stranded DNA (anti-ssDNA) antibodies were measured by ELISA using plates precoated with ssDNA. Anti-chromatin antibodies were measured by ELISA using plates that had been coated with double-stranded DNA and total histone solution (Sigma Chemical). Standard units were derived using serial dilution of an anti-nuclear antibody (ANA)-positive NZM2410 serum pool.

1. Lim A, et al. (2002) Combination of MHC-peptide multimer-based T cell sorting with the immunoscope permits sensitive ex vivo quantitation and follow-up of human $CD8^+$ T cell immune responses. *J Immunol Methods* 261:177–194.

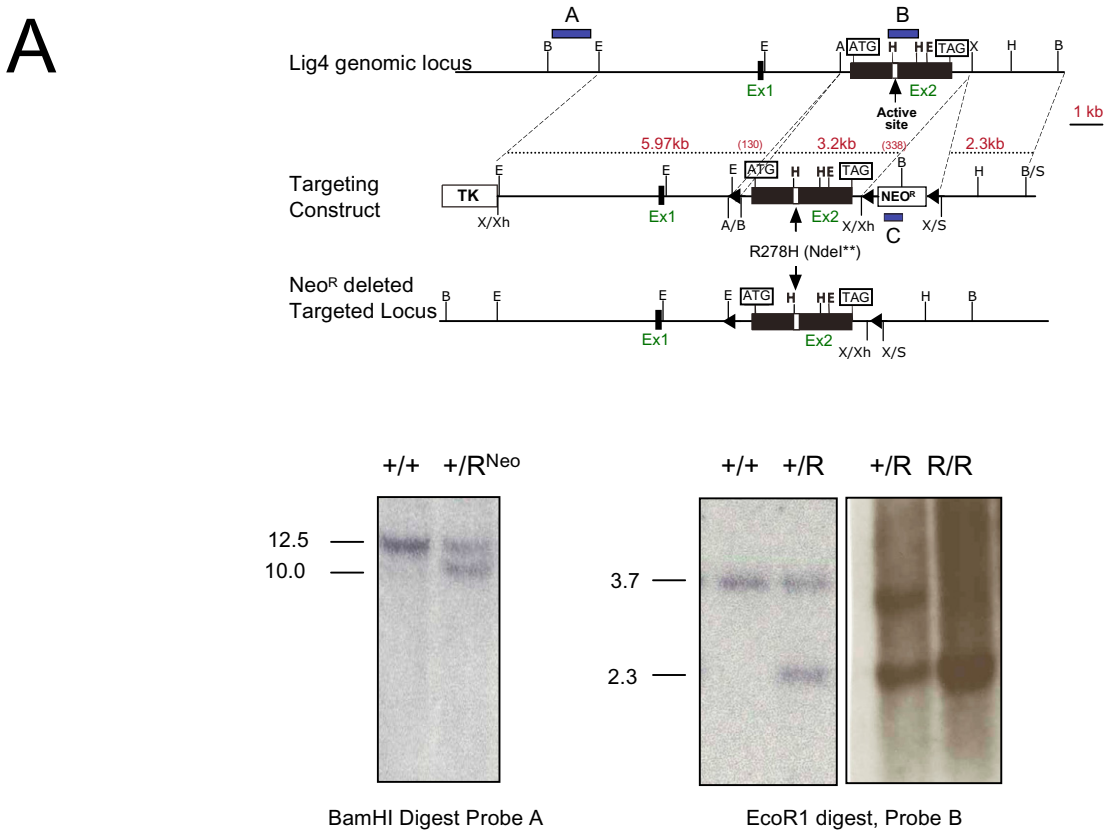

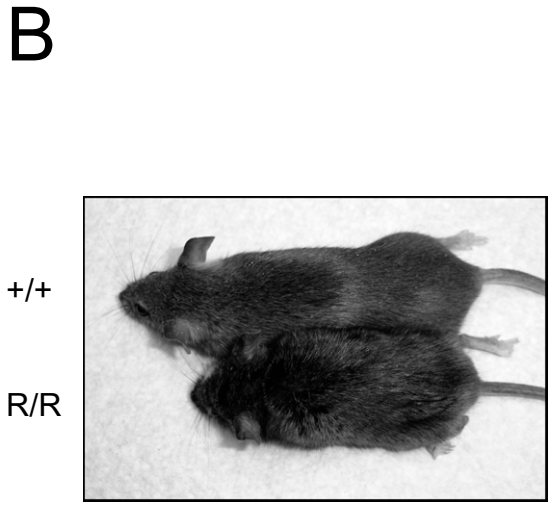

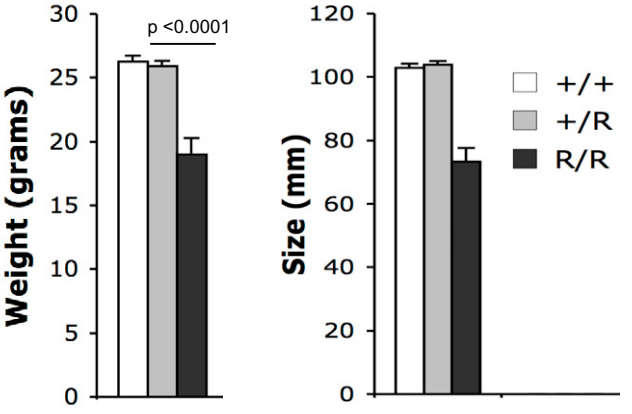

Fig. S1. Targeting strategy at the *Lig4* locus. (*A*) (*Upper*) Schematic of targeting construct and Southern blot analysis of sequentially targeted ES clones. *Top*, organization of the *Lig4* genomic locus and probes used. *Middle*, targeting construct with CGC to CAT nucleotide change at codon 278, leading to arginine (R) 278 to histidine (H) mutation in the catalytic active site of the protein. A novel NdeI** restriction site created by the R278H mutation is shown. The final R278H targeting construct consists of two *Lig4* gene genomic fragments: a 9.17-kb XbaI 5′ arm containing both *Lig4* gene exons 1 and 2 blunted by a Klenow fragment and cloned into the XhoI site of the pLNTK targeting vector and a 2.3-kb XbaI-BamHI fragment (3′ arm) that was blunted by a Klenow fragment and cloned into the SalI site of pLNTK. We generated the R278H targeting construct such that the *Lig4* gene could if needed also be conditionally inactivated by Cre recombinase by flanking *Lig4* exon 2 with loxP sites. The 5′ loxP, which is contained within a 100-bp BamHI fragment with a unique EcoRI site, was blunt-end ligated into the AflII site 130 bp upstream of the exon 2 ATG. The 3′ loxP site, which flanks the neomycin resistance (Neo^R) gene in pLNTK, resides 338 bp downstream of the *Lig4* gene TAG stop codon. The distances between the loxP sites that flank *Lig4* exon 2 and the ATG translation initiation site and the TAG

Legend continued on following page

stop codon are shown in parentheses. *Bottom*, targeted locus with Neo^R marker deleted. A, AflII; B, BamHI; E, EcoRI; H, HindIII; S, SacI; X, XbaI; Xh, XhoI. —, 1-kb bar. (*Lower*) Southern blot of BamHI (left) or EcoRI (right)-digested ES cell genomic DNA, probed with probes A and B, respectively, was used to detect wild-type (+/+), heterozygous (+/R), and homozygous (R/R) bands. For sequential targeting in ES cells, probe C (shown in *A*) was used to identify +/R^{Neo} and R/ R^{Neo} ES cells that were then infected with the Cre-recombinase to obtain +/R and R/R ES cells, respectively. Southern blotting using EcoRI (right)-digested ES cell genomic DNA was then probed with probe B to detect the germline 3.7-kb and the mutant (R) 2.3-kb bands and with probe C to detect loss of the Neo^R gene. (*B*) +/+ and R/R littermates are compared side by side at 4 months of age. R/R mice display significant growth retardation compared with +/+ and +/R littermates. (*C*) Weight and size (mean ± SE) of 20-week-old +/+ (n = 10), +/R (n = 10), and R/R (n = 10) littermates. *P* values were determined by unpaired Student's *t* test.

A

	Cell line	(Amp^R+Cam^R)/Amp^R	Percentage	Relative level
Exp1	TC1	244/206,600	0.1181	
	Lig4$^{R/R}$	9/313,000	0.00288	0.0246
	Lig4$^{-/-}$	18/376,200	0.00478	0.04053
Exp2	TC1	1,300/364,000	0.3571	
	Lig4$^{R/R}$	8/203,000	0.00394	0.0109
	Lig4-/-	4/440,000	0.00091	0.00254
Exp3	TC1	402/213,400	0.1883	
	Lig4$^{R/R}$	3/81,000	0.003703	0.0196
	Lig4$^{-/-}$	3/103,700	0.00289	0.01535

B

RS Joins recovered from Lig4$^{R/R}$ ES cells

	Left RS Flank	N	Right RS Flank		# Clones
	GTTTTTGTTCCAGTCTGTAGCACTGTG		CACAGTGGTAGTACCTCCACTGTCTGGCTGTACAAAAACC		
0	GTTTTTGTTCCAGTCTGTAGCACTGTG		CACAGTGGTAGTACCTCCACTGTCTGGCTGTACAAAAACC	0	14
0	GTTTTTGTTCCAGTCTGTAGCACTGTG			-40	1
0	GTTTTTGTTCCAGTCTGTAGCACTGTG	GTAGTA	CTCCACTGTCTGGCTGTACAAAAACC	-14	1
-7	GTTTTTGTTCCAGTCTGTAG	TA	CTCCACTGTCTGGCTGTACAAAAACC	-14	1
-16	GTTTTTGTTCC		CTCCACTGTCTGGCTGTACAAAAACC	-14	1
-16	GTTTTTGTTCC			-40	1
-27			CTCCACTGTCTGGCTGTACAAAAACC	-14	1
-15	GTTTTTGTTCCA	248bp insertion	AAAAACC	-33	1

RS Joins recovered from TC1 ES cells

	Left RS Flank	N	Right RS Flank		# Clones
	GTTTTTGTTCCAGTCTGTAGCACTGTG		CACAGTGGTAGTACCTCCACTGTCTGGCTGTACAAAAACC		
0	GTTTTTGTTCCAGTCTGTAGCACTGTG		CACAGTGGTAGTACCTCCACTGTCTGGCTGTACAAAAACC	0	27

Fig. S2. Analysis of RS joins in Lig4$^{R/R}$ ES cells. (*A*) Analysis of RS joins from three independent experiments. (*B*) Sequence analysis of V(D)J RS joins (pJH200) recovered from *Lig4*$^{R/R}$ and wild-type TC1 ES cells in V(D)J recombination assays. The fidelity of the RS joins was determined by PCR amplification of the pJH200 segment and digestion of the products with ApaLI. Individual Amp^R+Cam^R clones were isolated and sequenced. Germline sequences are shown in the first row. Nucleotides that cannot be unequivocally assigned to either flanking end are shown in the center. The number in the right column (# clones) indicates the number of identical sequences recovered from the various transfection experiments.

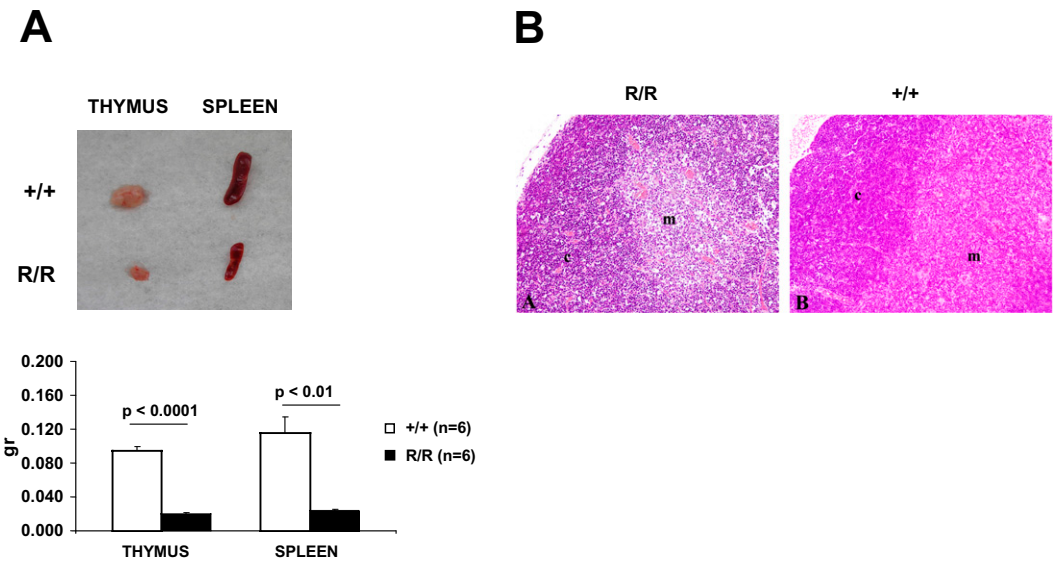

Fig. S3. *Lig4*$^{R/R}$ mice have hypoplastic thymus and spleen and show mild thymic alterations with conserved architecture and corticomedullary differentiation. (*A*) (*Upper*) Comparison of thymus and spleen of wild-type (+/+) versus *Lig4*$^{R/R}$ (R/R) mice. (*Lower*) Weight of thymus and spleen in +/+ and R/R mice. Weight in grams (gr) is shown as mean ± SE. (*B*) Hematoxylin/eosin staining of thymic sections from of a representative R/R mouse (*A*) shows mild architectural abnormalities with conserved demarcation between the cortex (c) and the small-sized medulla (m). Architecture of the thymus from a littermate control is shown for comparison (*B*). (Magnification, 10×.)

Coding joins

Vbeta 14 coding sequence	P/N	Dbeta 1 segment	P/N	Jbeta1.1 sequence	FRAME	No. of deleted nts
CTCTGGCTTCTACCTCTGTGCCTGGAGTCT		GGGACAGGGGC		CAAACACAGAAGTCTTCTTTGGTAAAGGAAC		
+/+						
CTCTGGCTTCTACCTCTGTGCCTGGAGTCT	CCA	GGGAC	GGA	ACAGAAGTCTTCTTTGGTAAAGGAAC	NP	4
CTCTGGCTTCTACCTCTGTGCCTGGAGTCT	CA	GGACAG	A	AAACACAGAAGTCTTCTTTGGTAAAGGAAC	P	1
CTCTGGCTTCTACCTCTGTGCCTGGAGTCT	AT	CAGGGG	GCTGT	ACACAGAAGTCTTCTTTGGTAAAGGAAC	NP	3
CTCTGGCTTCTACCTCTGTGCCTGGAGTCT	CCT	C	G	CAAACACAGAAGTCTTCTTTGGTAAAGGAAC	P	0
CTCTGGCTTCTACCTCTGTGCCTGGAGTCT	TTAAA	GGGC	C	CAAACACAGAAGTCTTCTTTGGTAAAGGAAC	NP	0
CTCTGGCTTCTACCTCTGTGCCTGGAGTCT	CCACGG	AGGGG		ACACAGAAGTCTTCTTTGGTAAAGGAAC	P	3
CTCTGGCTTCTACCTCTGTGCCTGGAGTCT	A	AGGGG	TGGC	ACACAGAAGTCTTCTTTGGTAAAGGAAC	NP	3
CTCTGGCTTCTACCTCTGTGCCTGGAGTCT	TTAA	AGGG	CC	CAAACACAGAAGTCTTCTTTGGTAAAGGAAC	NP	0
CTCTGGCTTCTACCTCTGTGCCTGGAGTC	CCCCC	GGGACAG		CAAACACAGAAGTCTTCTTTGGTAAAGGAAC	P	1
CTCTGGCTTCTACCTCTGTGCCTGGAG	CACGTATC	GGA	GA	AAACACAGAAGTCTTCTTTGGTAAAGGAAC	NP	4
CTCTGGCTTCTACCTCTGTGCCTGGAG	CGGT	ACAGG		GAAGTCTTCTTTGGTAAAGGAAC	P	11
CTCTGGCTTCTACCTCTGTGCCTGGAG	GCA	ACAG	AA	CAAACACAGAAGTCTTCTTTGGTAAAGGAAC	NP	3
CTCTGGCTTCTACCTCTGTGCCTGGAG	CCG	CAGGGG		AAACACAGAAGTCTTCTTTGGTAAAGGAAC	P	4
CTCTGGCTTCTACCTCTGTGCCTGGAG		AGG	TG	CAAACACAGAAGTCTTCTTTGGTAAAGGAAC	P	3
CTCTGGCTTCTACCTCTGTGCCTGG	GA	GGGACAG		CAAACACAGAAGTCTTCTTTGGTAAAGGAAC	P	5
R/R						
CTCTGGCTTCTACCTCTGTGCCTGGAGTCT	G	GGGGC	AC	ACACAGAAGTCTTCTTTGGTAAAGGAAC	P	3
CTCTGGCTTCTACCTCTGTGCCTGGAGTCT		GGACAGG		GAAGTCTTCTTTGGTAAAGGAAC	P	8
CTCTGGCTTCTACCTCTGTGCCTGGAGTCT		AGG	C	AACACAGAAGTCTTCTTTGGTAAAGGAAC	P	2
CTCTGGCTTCTACCTCTGTGCCTGGAGTCT		AGGG		ACAGAAGTCTTCTTTGGTAAAGGAAC	P	5
CTCTGGCTTCTACCTCTGTGCCTGGAGTC	GGGAGC	CAGGG		GAAGTCTTCTTTGGTAAAGGAAC	P	9
CTCTGGCTTCTACCTCTGTGCCTGGAGTC		CA	AC	CACAGAAGTCTTCTTTGGTAAAGGAAC	P	5
CTCTGGCTTCTACCTCTGTGCCTGGAG	GGG	AGGGG	GCGCG	AACACAGAAGTCTTCTTTGGTAAAGGAAC	P	5
CTCTGGCTTCTACCTCTGTGCCTGGAG		GA	A	AAACACAGAAGTCTTCTTTGGTAAAGGAAC	P	7
CTCTGGCTTCTACCTCTGTGCCTGGAG		GGA		AGAAGTCTTCTTTGGTAAAGGAAC	P	10
CTCTGGCTTCTACCTCTGTGCCTGGA	CCTACA	AG		CAAACACAGAAGTCTTCTTTGGTAAAGGAAC	P	4
CTCTGGCTTCTACCTCTGTGCCTGGA				CAAACACAGAAGTCTTCTTTGGTAAAGGAAC	P	4
CTCTGGCTTCTACCTCTGTGCCTGGA		CAG		CAGAAGTCTTCTTTGGTAAAGGAAC	P	10
CTCTGGCTTCTACCTCTGTGCCTGG	T	GGA	A	AAACACAGAAGTCTTCTTTGGTAAAGGAAC	P	6
CTCTGGCTTCTACCTCTGTGCCTGG	GGG	GGGG	GTT	CAAACACAGAAGTCTTCTTTGGTAAAGGAAC	P	5
CTCTGGCTTCTACCTCTGTGCCTGG		C		AAGTCTTCTTTGGTAAAGGAAC	P	14
CTCTGGCTTCTACC	GGTG	CAGGGG	G	CAAACACAGAAGTCTTCTTTGGTAAAGGAAC	NP	16

RS joins

Dbeta1 RSS	"N"	Vbeta 14 RSS	Number of clones	deletions	insertions
CTTTTTTGTATAAAGCTGTAACATTGTG		CACACTGAGTAGGGTGGGGCAGACATCTGTGCAAAAACC			
+/+					
CTTTTTTGTATAAAGCTGTAACATTGTG		CACACTGAGTAGGGTGGGGCAGACATCTGTGCAAAAACC	23	0	0
CTTTTTTGTATAAAGCTGTAACATTGTG	GG	CACACTGAGTAGGGTGGGGCAGACATCTGTGCAAAAACC	2	0	2
CTTTTTTGTATAAAGCTGTAACATTGTG	CC	CACACTGAGTAGGGTGGGGCAGACATCTGTGCAAAAACC	2	0	2
CTTTTTTGTATAAAGCTGTAACATTGTG	GT	CACACTGAGTAGGGTGGGGCAGACATCTGTGCAAAAACC	1	0	2
CTTTTTTGTATAAAGCTGTAACATTGTG	ACG	CACACTGAGTAGGGTGGGGCAGACATCTGTGCAAAAACC	1	0	3
CTTTTTTGTATAAAGCTGTAACATTGTG	GGG	CACACTGAGTAGGGTGGGGCAGACATCTGTGCAAAAACC	1	0	3
CTTTTTTGTATAAAGCTGTAACATTGTG	GGGGT	CACACTGAGTAGGGTGGGGCAGACATCTGTGCAAAAACC	1	0	5
R/R					
CTTTTTTGTATAAAGCTGTAACATTGTG		CTGAGTAGGGTGGGGCAGACATCTGTGCAAAAACC	1	4	0
CTTTTTTGTATAAAGCTGTAACATTGT	CC	CTGAGTAGGGTGGGGCAGACATCTGTGCAAAAACC	1	5	2
CTTTTTTGTATAAAGCTGTAACATTG		GGGTGGGGCAGACATCTGTGCAAAAACC	2	13	0
CTTTTTTGTATAAAGCTGTAA		GGGGCAGACATCTGTGCAAAAACC	3	22	0
CTTTTTTGTATAAAGCTGT		AACC	2	44	0
CTTTTTTGTATAAAGCTGT	CGG	GTAGGGTGGGGCAGACATCTGTGCAAAAACC	2	17	3
CTTTTTTGTATAAAGCTGT	CC	CACACTGAGTAGGGTGGGGCAGACATCTGTGCAAAAACC	1	9	2
CTTTTTTGTATAAAGCTGT	GGCATTGGG	AGACATCTGTGCAAAAACC	1	29	9
CTTT		GGTGGGGCAGACATCTGTGCAAAAACC	1	35	0
CTT	C	GGTGGGGCAGACATCTGTGCAAAAACC	1	36	1
(-35bp from the CTTTT)		(-65bp from the CACA)	1	166	0
(-12bp from the CTTTT)		(-41bp from the CACA)	1	119	0

Fig. S4. *Lig4*$^{R/R}$ thymocytes show largely preserved coding joins formation, but imprecise RS joins. (*Upper*) Comparison of Vβ14-Dβ1-Jβ1.1 rearrangements in thymocytes from *Lig4*$^{+/+}$ (+/+) and *Lig4*$^{R/R}$ (R/R) mice. The germline sequence of the Vβ14, Dβ1, and Jβ1.1 segments is shown at the top. Individual clones with productive (P) and nonproductive (NP) rearrangements are shown, with P/N nucleotide insertions. The number of deleted nucleotides is shown in the right column. Boxes identify areas of microhomology. (*Lower*) RS joins sequences in thymocytes from +/+ and R/R mice, following Vβ14-Dβ1 rearrangement. The number of individual clones showing each sequence is shown. RS joins in R/R mice are characterized by extensive deletions.

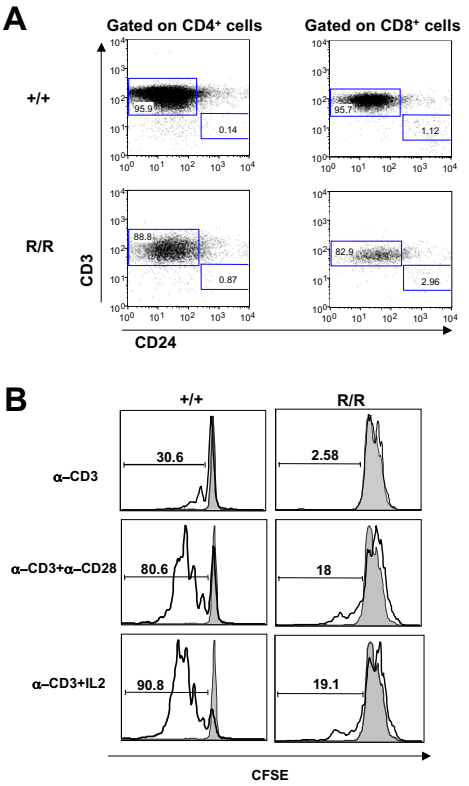

Fig. S5. Splenic T cells from *Lig4*$^{R/R}$ mice have a mature phenotype and show decreased in vitro proliferation. (*A*) CD4^{+} and CD8^{+} splenic T cells from *Lig4*$^{R/R}$ (R/R) and control (+/+) mice (n = 3 per group) were stained for CD3 and CD24. The proportion of mature (CD3^{hi} CD24^{lo}) and immature (CD3^{lo} CD24^{hi}) cells is shown. (*B*) Representative example of proliferation of R/R and +/+ splenic T cells, cultured in the presence of anti-CD3, anti-CD3 plus anti-CD28, or anti-CD3 plus IL-2. Proliferation was assessed by CFSE dilution, gating on live cells. Solid histograms represent unstimulated cells.

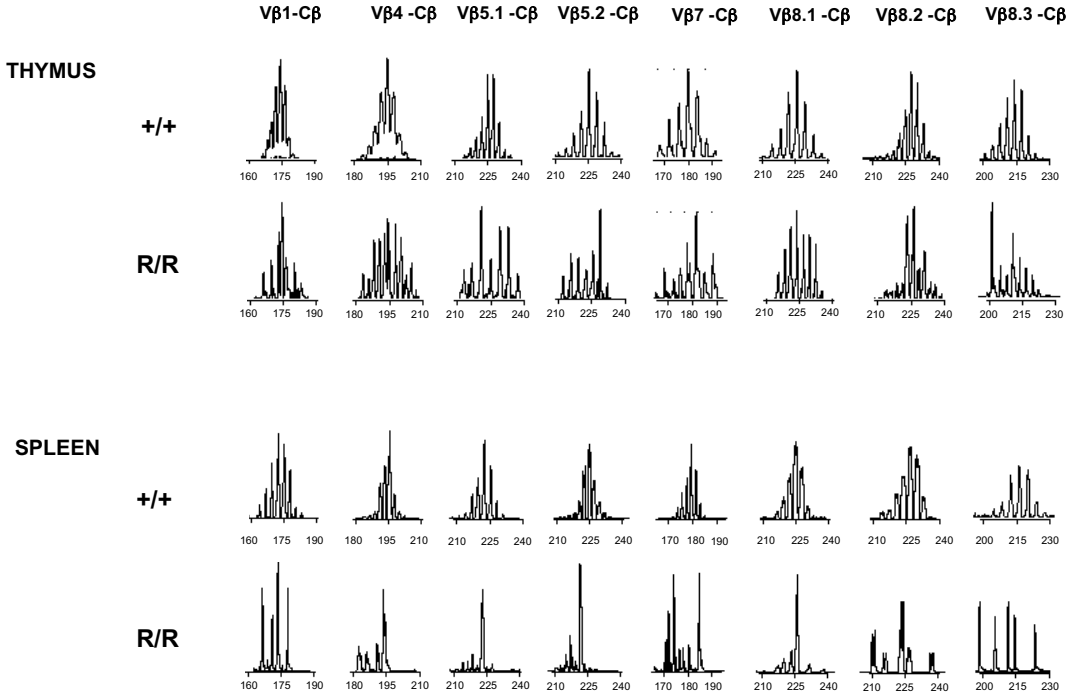

Fig. S6. *Lig4*$^{R/R}$ mice have a largely polyclonal T cell receptor (TCR) Vβ repertoire in the thymus, but a restricted TCR Vβ repertoire in the spleen. Immunoscope profile is shown of thymocytes and CD90^{+} splenic T cells from 5-week-old *Lig4*$^{R/R}$ (R/R) and *Lig4*$^{+/+}$ (+/+) mice. The CDR3 length distribution profile is shown for 8 TCR Vβ-Cβ amplification products. The CDR3 length is shown on the x axis, and fluorescence intensity of the runoff products is reported on the y axis. Skewed distribution of CDR3 lengths is indicative of a restricted TCR Vβ repertoire. Profiles are shown for 8 of the 24 distinct TCR Vβ-Cβ amplification products analyzed. Each spectratype profile is representative of replicates in at least three animals.

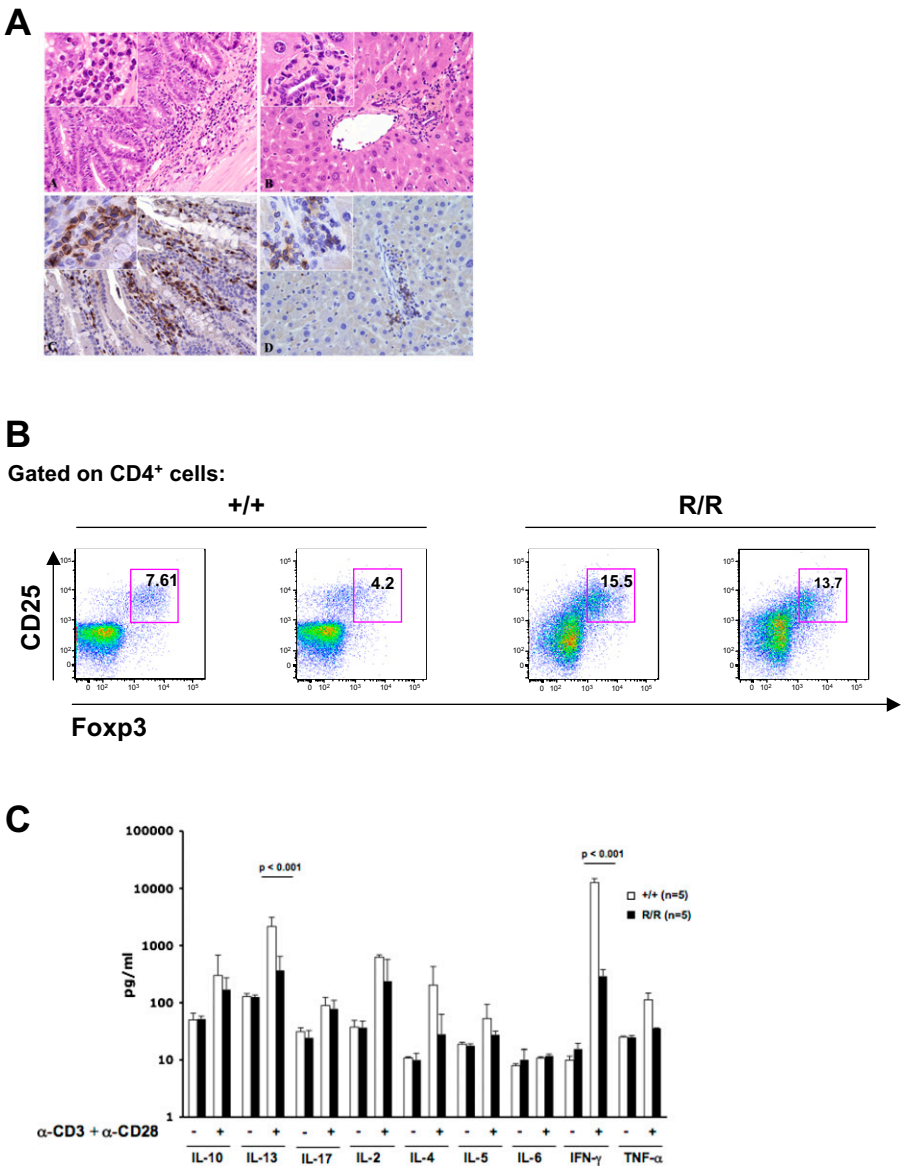

Fig. S7. Modest peripheral inflammatory infiltrates, presence of regulatory T cells, and in vitro T cell-mediated cytokine production profile in *Lig4*$^{R/R}$ mice. (*A*) Histological analysis of the gut of a *Lig4*$^{R/R}$ (R/R) mouse revealed only mild inflammatory infiltrates (*A*, hematoxylin/eosin staining) that were mainly composed of T lymphocytes (*C*, CD3 staining) and granulocytes (*A Inset*). Similarly, mild inflammatory infiltrates were found in the liver portal tracts (*B*, hematoxylin/eosin staining), with similar cellular composition (*B* and *D Insets*). Staining in *Insets* of *C* and *D* is for CD3 expression. [Original magnification: 20× (40× for *Insets*).] Data shown are from one representative 8-week-old R/R mouse of six that were analyzed. (*B*) Staining for regulatory T cells (CD4$^+$ CD25^{hi} Foxp3$^+$) in mesenteric lymph nodes from 8-week-old R/R and *Lig4*$^{+/+}$ (+/+) mice ($n = 2$ per group). (*C*) Levels of cytokines in the supernatants of R/R and +/+ splenic T cells, cultured with anti-CD3 and anti-CD28 mAbs for 72 h. Results are represented as mean ± SD, and *P* values were determined by two-way ANOVA test.

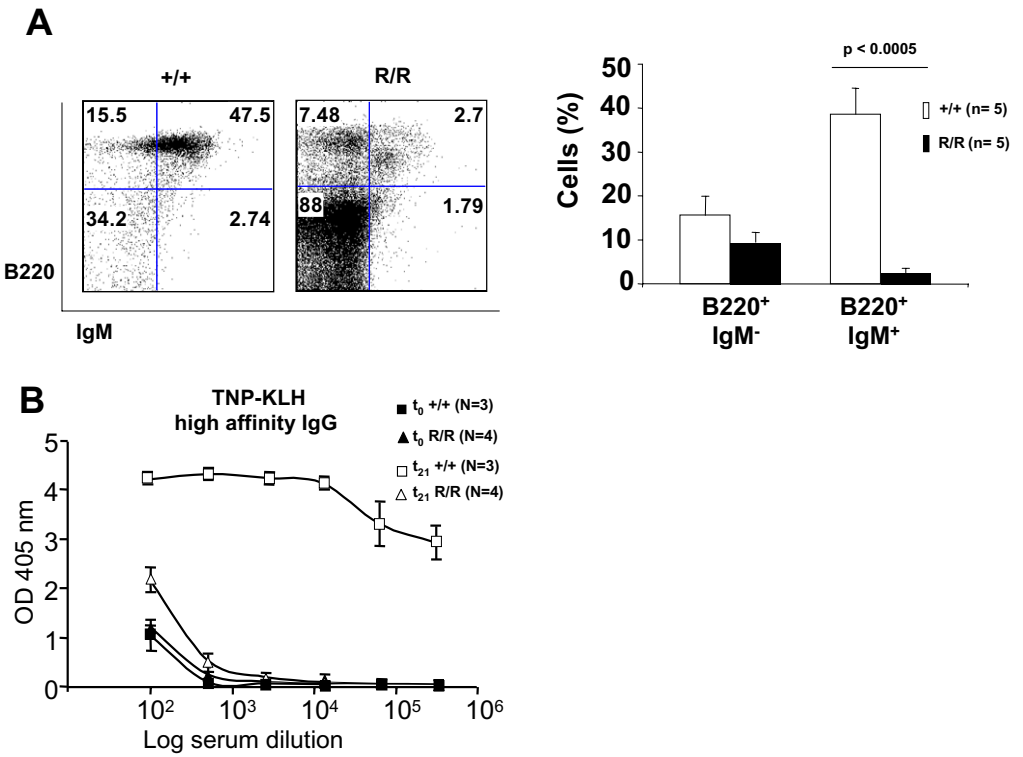

Fig. S8. Severe deficiency of mature splenic B cells and lack of production of high-affinity antibodies in response to the T-dependent antigen TNP-KLH in *Lig4*$^{R/R}$ mice. (*A*) Dot plot analysis of splenocytes labeled with B220 and IgM antibodies (*Left*) and representation of the percentages (± SE) of B220^{+} IgM^{-} and B220^{+} IgM^{+} splenocyte subpopulations (*Right*) in wild-type (+/+) and *Lig4*$^{R/R}$ (R/R) mice, upon gating on mononuclear cells. *P* values were determined by unpaired Student's *t* test. (*B*) Levels of high-affinity IgG antibodies to TNP(2) before immunization (t_0) and 7 days after secondary immunization (t_{21}) with TNP-KLH in +/+ and R/R mice.

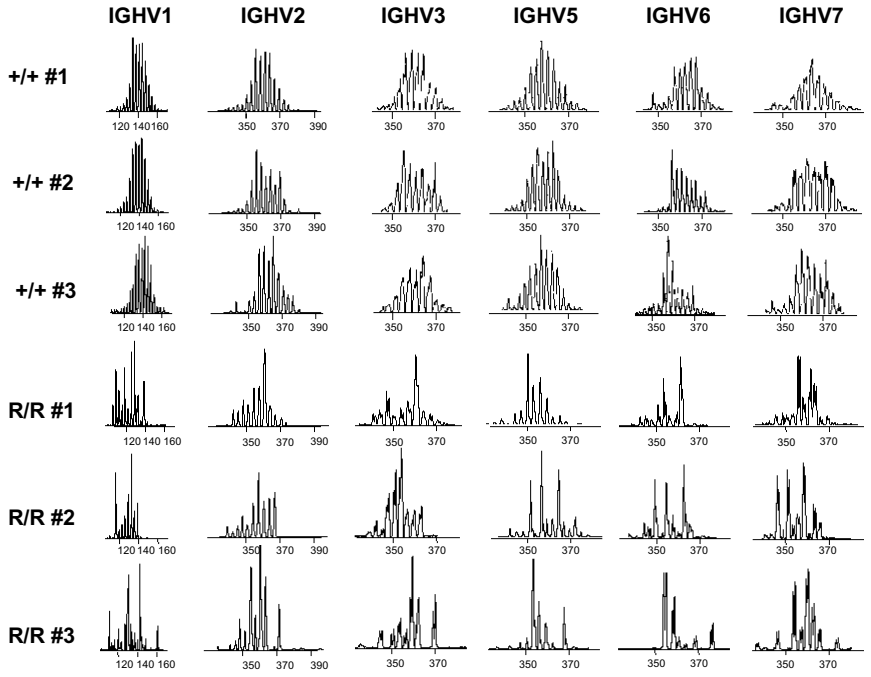

Fig. S9. Restricted B-cell repertoire in *Lig4*$^{R/R}$ mice. Immunoscope profile is shown in splenocytes of 5-week-old *Lig4*$^{R/R}$ (R/R) and *Lig4*$^{+/+}$ (+/+) mice (n = 3 for both groups). The CDR3 length distribution profile is shown of six Ig heavy chain VH families. The CDR3 length is shown on the *x* axis and fluorescence intensity of the runoff products is reported on the *y* axis.